Nat. Hazards Earth Syst. Sci. Discuss., 2, 7269–7292, 2014
www.nat-hazards-earth-syst-sci-discuss.net/2/7269/2014/
doi:10.5194/nhessd-2-7269-2014

Natural Hazards and Earth System Sciences
Open Access
Discussions

Linking local wildfire dynamics to pyroCb development

R. H. D. McRae[1], J. J. Sharples[2], and M. Fromm[3]

[1]Australian Capital Territory Emergency Services Agency, Canberra, Australia
[2]University of New South Wales, Canberra, Australia
[3]US Naval Research Laboratory, Washington, USA

Received: 17 September 2014 – Accepted: 11 October 2014 – Published: 2 December 2014

Correspondence to: R. H. D. McRae (rick.mcrae@act.gov.au)

Published by Copernicus Publications on behalf of the European Geosciences Union.

Abstract

Extreme wildfires are global phenomena that consistently result in loss of life and property, and further impact the cultural, economic and political stability of communities. In their most extreme form they cause widespread devastation of environmental assets and are capable of impacting the upper troposphere–lower stratosphere through the formation of a thunderstorm within the plume. Such fires are now often observed by a range of remote sensing technologies, which together allow a greater understanding of a fire's complex dynamics.

This paper considers one such fire that burnt in the Blue Mountains region of Australia in late-November 2006, that is known to have generated significant pyrocumulonimbus clouds in a series of blow-up events. Observations of this fire are analysed in detail to investigate the localised processes contributing to extreme fire development. In particular, it has been possible to demonstrate for the first time that the most severe instances of pyroconvection were driven by, and not just associated with, extreme local fire dynamics, especially the fire channelling phenomenon, which arises due to an interaction between an active fire, local terrain attributes and critical fire weather, and causes the fire to rapidly transition from a frontal to an areal burning pattern. The impacts of local variations in fire weather and of the atmospheric profile are also discussed, and the ability to predict extreme fire development with state-of-the-art tools is explored.

1 Introduction

Over the last decade southeastern Australia has experienced a number of extreme wildfire events. These include the January 2003 Alpine Fires (Nairn, 2003), the 2006–2007 Great Divide Fires (Smith, 2007) and the 2009 Victorian Fires (Teague et al., 2010), and also multiple fires in more recent years that are still under review. These fires caused widespread destruction of assets (both natural and anthropogenic)

NHESSD
2, 7269–7292, 2014

and multiple fatalities. While such fires are undoubtedly tragic, they do offer rare opportunities to better understand the dynamics and impacts of extreme wildfires. Of particular interest in this context is the development of pyroconvective plumes that inject smoke and other wildfire emissions high into the atmosphere.

The development of these extreme plumes, which manifest as pyrocumulus or pyrocumulonimbus (pyroCb) (American Meteorological Society, 2013), signals a transition in fire development from what is primarily a surface phenomenon to a coupled fire-atmosphere phenomenon (Potter, 2002; McRae and Sharples, 2011), in which the fire is able to interact with upper levels of the atmosphere (i.e. the mixed layer and above). Fires which make such a transition may access stronger winds and very dry air, which if returned to the surface (e.g. through convective mixing) can lead to extreme levels of fire behaviour and rates of spread (Potter et al., 2007; Mills, 2005, 2008). These fires would therefore be extremely difficult to suppress and would be very likely to do extensive damage to any assets they impacted (McRae and Sharples, 2011).

The injection height of smoke plumes from wildfires also has direct bearing on the effects of smoke and other emissions on air quality and climate, as it is a major factor governing downwind dispersal (Jost et al., 2004; Mazzoni et al., 2007; Kahn et al., 2008). In the most extreme instances of pyroconvection, emissions from wildfires can be injected into the lower stratosphere with subsequent global-scale impacts on atmospheric chemistry (Fromm et al., 2004; Trentmann et al., 2006; Rosenfeld et al., 2007). Stratospheric injection of pyrogenic aerosols could also play an important part in the interaction between wildfire occurrence and climatic warming (Fromm et al., 2004; Jost et al., 2004). Large fire plumes offer a direct transport path between the planetary boundary layer and the stratosphere, which is not fully captured by large-scale atmospheric transport models (Jost et al., 2004).

In their analysis of the 2003 Canberra bushfires, Sharples et al. (2012) demonstrated several cases where interactions between strong winds and rugged topography resulted in rapid wildfire development. The resulting process, which they termed “fire channelling”, resulted in a transition from the usual frontal burning pattern to an areal burning pattern caused by a combination of rapid lateral fire propagation (transverse to the prevailing winds) and downwind in-fill by short- to medium-range spotting. In one instance, they tenuously linked the fire channelling phenomenon to the development of a towering pyroCb that reached a height of some 15 km a.g.l. (Fromm et al., 2006; Sharples et al., 2012).

Such pyroCb events are at the most extreme end of the pyroconvective scale. Indeed such high level smoke injection events hardly feature at all in previous studies of fire plumes (e.g. Lavoue et al., 2000; Val Martin et al., 2010). Fromm et al. (2010) discuss the global climatology of pyroCb events, and note in particular the small number of published studies. Since 2001 there have been at least 30 instances of significant pyroCb occurrence in Australia either demonstrated or inferred from their injection of aerosols into the UTLS (Tables A1 and A2). While there is the possibility that additional pyroCbs have occurred in the past in association with significant bushfires that predate the technology necessary to formally detect them, the recent frequency of pyroCb occurrence in Australia is surprising.

Fromm et al. (2012) analysed pyroCb occurrence associated with two of the fires that occurred in eastern Australia during the spring and summer of 2006/2007, at locations shown in Fig. 1a. The so-called Grose Valley and Wollemi fires were notable due to the fact that they blew-up quasi-simultaneously in the late morning, rather than in the late afternoon when blow-ups typically occur (Fromm et al., 2010). Based on remotely sensed data from a range of satellites and weather radar, and surface and profile data from official weather observation sites, Fromm et al. (2012) concluded that the factors of significance for the development of the pyroconvection were anomalous boundary layer sensible heat and wind speed. They also noted that neither factor alone was deterministic, and that there was a clear need to further scrutinise the local drivers of the extreme fire behaviour.

The present paper therefore extends the study of Fromm et al. (2012) by exploiting data recorded for the Grose Valley Fire by an airborne multispectral linescanner (Cook et al., 2009), which provides critical insights into the wildfire dynamics. The combination of time-stamped, spatially-rectified fire data and radar data (local convective intensity, vertically aggregated convective intensity and plume top height) permits detailed examination of the fire's development and the localised pyroconvective contributions. Moreover, the combined analyses permit further scrutiny of the role of dynamic fire processes, such as mass spotting and the fire channelling phenomenon, in extreme fire development. In particular, the link between fire channelling and pyroCb development, which hitherto was established in only a single instance and in only a very qualitative way, is examined in greater depth and in more quantitative detail.

2 Data

It should be noted that all times (and thus dates) used in this paper are in UTC. Local time, Australian Eastern Summer Time, is UTC plus 11 h.

2.1 Satellite data

An initial examination of the areas of intense fire activity was conducted on LANDSAT archival imagery from USGS. One image that is both relatively cloud-free and free of scan-line correction problems showed the post-fire scars. An excerpt of the image is shown in Fig. 1d, and clearly indicates leafless eucalypt canopy left behind by intense fire activity.

As described in Fromm et al. (2012), much of the broad understanding of these fires derives from data acquired by the "A-Train" environment monitoring satellite flotilla.

2.2 Weather data

Weather data were supplied by the Australian Bureau of Meteorology (BoM). This included automatic weather station (AWS) half-hourly observations and daily vertical profiles from radiosonde flights. Relevent weather data were recorded at Mt Boyce AWS (WMO Station Number 94743), Nullo Mountain AWS (94754), Penrith Lakes AWS

NHESSD
2, 7269–7292, 2014

(94763) and Cessnock Airport AWS (95771), and radiosonde data were recorded at Williamtown (94776). The radar data were recorded by the Newcastle radar. The locations of all of the above recording stations are shown in Fig. 1a.

Figure 2 shows time series plots of key weather measurements and fire indices for these stations. Fire behaviour estimates, using the equations of Noble et al. (1980), are based on the Forest Fire Danger Index (FFDI). As no direct measurements of fuel moisture content (FMC) were available, FMC was described using the dimensionless fuel moisture index (FMI), which has been shown to produce reliable estimates of fuel moisture content in a variety of fine fuel types (Sharples et al., 2009; Sharples and McRae, 2011; Sharples and Matthews, 2011). In particular, Sharples et al. (2009) showed that FMI ≤ 5 consistently corresponded to eucalypt litter moisture contents below 3–4 %, a predictor of elevated fire intensity.

2.3 Radar data

The reflectivity data forming a full volume scan are available at 10 min resolution over 22 November. Computations from scan elevations and range permit estimation of the maximum height of radar returns (the "echotop") (Fromm et al., 2012). We also employ vertical aggregated reflectivity, an indication of overall convective activity. The aggregation is performed between the lowest elevation scan and the nominal cloud-base altitude (taken to be 4 km, based on the local radiosonde temperature and humidity profile at Williamtown). Echoes at these altitudes are attributable to non-hydrometeors such as debris lofted by the active fire (Lindley et al., 2011). Above the cloud-base stronger echoes are returned by hydrometeors, although these tend to be anomalously small (Rosenfeld et al., 2007).

2.4 Multispectral linescan data

The New South Wales Rural Fire Service aircraft used the Daedalus 1268 ATM multispectral linescanner supplied by Air Target Services Pty Ltd under contract (Cook et al., 2009; Sharples et al., 2012). For each run, flown at heights of 7 to 8 km, data acquisition took generally 10 min to complete. In some cases a number of contiguous passes were merged to provide coverage of the whole fire area.

Indicative colour samples are provided in Fig. 3f, however they relate to dynamically calibrated multispectral linescan products, taken in varying smoke scattering and absorption environments, which alter the pseudo-colour rendering.

3 Results

The available data for the Grose Valley Fire allow detailed analysis of its dynamics. Figure 1b shows localities relevant to this. These are referred to using codes explained in the figure caption.

3.1 Fire spread prior to 21 November

The Grose Valley fire began as two ignitions generally 10 km north of Mt Boyce, which were detected on 14 November. The exact date and time of the ignitions are unknown (Cronstadt, 2006).

Prior to 02:07 21 November (linescan 116), the fire was spreading with a single bounding fireline (as seen in Fig. 3b) in a manner that could be deduced from fuel, terrain and weather data. It had gone out or been extinguished in places.

3.2 Breakout on 21 November

A breakout can be seen in Fig. 3b, north of AR. As a result of this, the containment line for the fire in the north-east had to be extended to the south-east of ER. Figure 3c shows this as cold edge (linescan 117 M, at 00:20 22 November), but also shows active fire edge extending past BR to the south-east.

The fire has burnt parallel to the cliffline and bypassed containment and become established on the plateau around ER, as might be expected, given the terrain and the low FMI inferred from the weather observations (Fig. 2b).

The fire slowed significantly on the steep downslope runs off the range at about 08:30 21 November, when the fire weather conditions began to ameliorate. At approximately this time the prevailing wind direction also changed from west-southwest to northwest (Mt Boyce, Fig. 2). The apparent lack of intense wind-driven fire activity at lower elevations in the Grose Valley suggests that these winds did not penetrate significantly down into the gorge; however, the fire on ER spread as a head-fire down BR. By 09:00 21 November this part of the fire complex had burnt approximately 350 ha, with some lesser runs later in the night indicated by radar returns.

3.3 Overnight foehn wind, 21 November

Observations at Penrith Lakes AWS indicated the presence of a pronounced foehn effect over parts of the region, starting at about 17:00 21 November, the night before the pyroCb blow-ups. Indeed, the synoptic weather pattern was consistent with that associated with the development of foehn winds in southeast Australia (Sharples et al., 2010). An abrupt increase in temperature from 21.4 to 30.3 °C with a complementary drop in relative humidity from 46 to 19 % was recorded over the period 16:30–17:00, 21 November at Penrith Lakes AWS (Fig. 2). Coincident with these changes was a change in wind direction from southwest to northwest and an increase in wind speed from 9 to about 30 km h^{-1}. This nocturnal foehn event would have significantly inhibited the usual moisture absorption by fuels that takes place overnight (Sharples, 2009; Sharples et al., 2010). It should be noted that while Mt Boyce AWS is close to the Grose Valley Fire, it is on part of the terrain that would be generating, not experiencing, the foehn effect. The easterly AWSs (Penrith Lakes and Cessnock) are where the full effects of adiabatic processes would be expected. The fire ground, being up to 800 m lower than Mt Boyce AWS, might be expected to experience the effects of such a foehn wind event.

The fire also spread to the south, from the end of the containment line near AR. At the white arrow in Fig. 3c the fire crossed a creek-line at the cliff-top and moved uphill towards the south. The fire also dropped below the cliff-line near CH and began to spread slowly downslope to the east towards Govetts Creek.

3.4 Widespread Spotting in Grose Valley, 22 November

Figure 3c also shows the fire crossing the Grose River, approximately 1.5 km WSW of MB, after backing down the slopes below AR and PL. At 01:00 22 November the wind at Mt Boyce AWS shifted towards the west and increased in speed to above 35 km h^{-1}. The change also brought the winds into closer alignment with the valley axis. Up until 02:41 22 November (linescan 126, Fig. 3d), the fire produced dense medium-range spot fires that extended 3.5 km downwind (in the area labelled "GV-C" in Fig. 1b), with a cross-wind extent of approximately 2 km. After merging, these spot fires covered an area of approximately 600 ha, as indicated in Fig. 3d. An extent of about 100 ha of this was on the plateau to the northwest of EDH, where the fire had merged with the right flank of the previous fire run over ER. Figure 3d shows that the entire area burnt with high intensity, based on the relatively uniform spectral signature for active or decaying flame (Fig. 3f).

3.5 Fire channelling, Banks Ridge, 22 November

At a similar time, the left flank of the fire on the plateau (near KGB and BR) exhibited spread with a notable northerly component, despite the west-northwest direction of the prevailing winds. This part of the fire complex is labelled "GV-N" in Fig. 1b. The relative intensity of the spectral signals indicates that this lateral spread produced more intense fire behaviour and higher rates of spread compared to that evident in Fig. 3c, two and a half hours earlier. The lateral fire propagation evident at GV-N is consistent with and best explained by the fire channelling phenomenon discussed by Sharples et al. (2012). Indeed, the steep lee slopes of the numerous side spurs leading north to CR satisfy

NHESSD
2, 7269–7292, 2014

the preconditions necessary for fire channelling to occur (Sharples et al., 2012). The downwind extension of the flaming zone extending towards MC is also consistent with that seen in other fire channelling events (Sharples et al., 2012).

There was a spatial alignment between the inferred fire channelling event at GV-N, which was captured at 02:41 22 November in Fig. 3d, and the strong radar returns recorded after 02:20 (Fig. 4b), the convective core of which has been outlined in Fig. 3d. Figure 4b indicates that the pyroconvective activity in the vicinity of GV-N started at approximately 01:30, and Fig. 4a shows that the pyroconvective top exceeded an altitude of 9 km for approximately 40 min between 02:30 and 03:10. This period covers that in which the intense lateral spread associated with fire channelling can be inferred to have been underway. This establishes a quantitative connection between the intense, lateral spread associated with fire channelling and the violent pyroconvective activity detected by the radar.

3.6 Fire Channelling, Clarke Head, 22 November

Figure 3e (linescan 127 M, 05:00 22 November) shows that, after traversing the heavily dissected cliff-line between PL and CH, the fire exhibited rapid lateral spread towards the south-southwest along a 1.3 km length of cliff-line. This part of the fire complex is labelled "GV-S" in Fig. 1b. The pattern of fire propagation depicted here is fully consistent with fire channelling and the terrain in this vicinity certainly meets the criteria necessary for fire channelling occurrence (Sharples et al., 2012). In addition to the lateral spread the fire also spread downwind for 2.6 km across Govetts Creek, producing an active flaming area of approximately 400 ha. This expanse of active flame was constrained at the cliff-line below DFH with some spotting for a further 1.7 km onto the plateau above. The southern flank of this part of the fire complex may be seen to be a series of merging spot fires, which is again consistent with other instances of fire channelling (Sharples et al., 2012).

The cross-wind dimension of the flaming zone depicted to the south-southwest of CH in Fig. 3e was 1.3 km, and assuming that the lateral spread was initiated immediately after 02:41, the inferred minimum rate of lateral spread is 0.6 km h^{-1}. However, it is unlikely that a spectral signature corresponding to active flaming (i.e. bright yellow) would persist for over 2 h without cooling and so it is far more likely that the fire covered the cross-wind distance over a time of the order of the burn-out time for the dominant vegetation type in the area, i.e. ∼ 30 min or less. Indeed, Fig. 4b indicates peak radar returns in the vicinity of GV-S sometime after 04:30, and if this is taken as an indicator of the onset of the lateral spread, then the estimate for the rate of lateral spread can be revised to 2.6 km h^{-1}. This latter estimate of the lateral rate of spread is of a similar order to that inferred in other cases of fire channelling using overlapping linescan data (Sharples et al., 2012).

Figure 3e illustrates the spatial alignment between the fire channelling event at GV-S and the location of the strong radar returns used to populate Fig. 4. Figure 4 indicates that this plume developed into a significant pyroCb that exceeded 9 km in height between 05:00 and 05:40. Moreover, Fig. 4a confirms that the radar detected an abrupt increase in the echotop altitude at approximately the same time as the fire channelling event at GV-S was underway. This extreme pyroCb activity associated with the fire channelling event ultimately registered echotops near the tropopause at ∼ 11.5 km.

4 Discussion and conclusions

Fromm et al. (2012) demonstrated that two fires in the hinterland of Sydney generated pyroCb clouds on 22 November 2006. Their broad analysis, which was based on satellite, radar and weather data indicated that the pyroCb occurrence was best reflected in the extreme value of the Continuous Haines Index (C-Haines), especially in its 850 hPa temperature component, and the surface winds, which reached high values earlier in the day than would typically be the case. These observations suggested that there was more to the escalation of these fires than the typical diurnal weather cycle.

NHESSD
2, 7269–7292, 2014

In this study we have shown that atypical modes of fire propagation, exacerbated by antecedent anomalous fire weather, driven by foehn wind occurrence, were a major factor in the pyroCb blow-ups.

Direct measurement of some of the important dynamics of a complex fire burning in a rugged landscape demonstrates that a variety of mechanisms may produce the required fire intensity for violent pyroconvection to commence, but that the most significant development of pyroCbs occurred in connection with the fire channelling phenomenon.

“Blow-up” has been used as a term for unexpected fire escalation and has been discussed at a technical level by Arnold and Buck (1954), Byram (1954), Steiner (1976) and McRae and Sharples (2013). Byram suggested that the wind profile is a contributor to blow-up potential. The vertical profile recorded at Williamtown (the closest relevant observation site) indicates a wind velocity maximum at about 1 km above the site elevation (a jet point, Byram, 1954), shown in Fig. 5.

Other work on blow-up fires has focussed on the role of vertical stability (Haines, 1988; Mills, 2008; Mills and McCaw, 2010). As discussed by Fromm et al. (2012), the C-Haines value was extreme during these events. Of relevance to the stability component of the C-Haines, a band of small dry thunderstorms that passed over the region on the afternoon of 22 November ignited new fires in the region of the Wollemi Fire by means of lightning strikes (NSW Rural Fire Service, 2006). Radar data shows that this band passed over the Grose Valley Fire at about 03:20 and the Wollemi Fire at 04:20. Figure 6 shows a radar image from 04:40.

The preceding analyses indicate that the forecast of the occurrence of a blow-up event needs to consider: the absence of a fine fuel moistening phase during the preceding night; the maximum fire danger at the surface, and its relation to the typical diurnal cycle; a jet point in the wind profile; the terrain on which the fire is burning (ruggedness) and its orientation to the prevailing wind; the time of arrival of fire in critical parts of the landscape; and the passage of atmospheric features that may exacerbate fire intensity. This is reflected in the model framework proposed by McRae and Sharples (2013).

NHESSD
2, 7269–7292, 2014

As pointed out by Fromm et al. (2012), the fire development on 21 November would have been subject to similar surface weather, terrain and fire behaviour features to that of 22 November. Moreover, there is only a subtle difference in the C-Haines between the two days. Thus, in terms of the tools normally applied by fire managers to such events, there may have been no substantial reason to expect the fundamentally different fire behaviour that was observed on 22 November.

While fire behaviour analyses based on fuel loads, surface weather and slope may be reconciled with a fire's ultimate extent, they cannot resolve the key processes described here. The demonstrated importance here of foehn winds, atypical fire propagation, wind profile and their association with pyroCb development provides a significant enhancement to our capability to mitigate the threats from extreme fires and blow-up events.

It should be noted that not all unexpected fire escalations are blow-up events as described above, but rather are likely to be due to poorly forecast surface weather or underestimated fuel loads. It is an increasingly important task of analysts investigating significant fires to determine the true nature of any escalations.

Acknowledgements. We thank: Tony Bannister, Bureau of Meteorology, for the level 2 radar data and AWS hourly surface observations; Laurence McCoy, NSW Rural Fire Service, for arranging access to the linescans (all linescans are courtesy of NSW Rural Fire Service GIS Section); Robert Norman, Air Target Services Pty Ltd; and David Crust, Area Manager, Mudgee, NSW National Parks and Wildlife Service.

References

American Meteorological Society: Glossary of Meteorology, available at: http://glossary.ametsoc.org/wiki/Pyrocumulonimbus (last acces: 24 April 2014), 2013.

Arnold, R. K. and Buck, C. C.: Blow-up fires – silviculture or weather Problems?, J. Forest., 52, 408–411, 1954.

Byram, G. M.: Atmospheric conditions related to blowup fires, Southeastern Forest Experimental Station Paper 35, Southeastern Forest Experimental Station, Asheville, NC, 1954.

Cook, R., Walker, A., and Wilkes, S.: Airborne fire intelligence, in: Innovations in Remote Sensing and Photogrammetry, edited by: Jones, S. and Reinke, K., Springer, Heidelberg, 239–254, 2009.

Cronstedt, M.: Lawson's long alley section 44 incident controller's report, Prepared for New South Wales Rural Fire Service, Sydney, New South Wales, 2006.

Fromm, M., Bevilacqua, R., Stocks, B., and Servranckx, R.: New directions: transport to the stratosphere: add fire-convection to volcanoes, Atmos. Environ., 38, 163–165, 2004.

Fromm, M., Tupper, A., Rosenfeld, D., Servrancx, R., and McRae, R.: Violent pyro-convective storm devastates Australia's capital and pollutes the stratosphere, Geophys. Res. Lett., 33, L05815, doi:10.1029/2005GL025161, 2006.

Fromm, M., Lindsey, D. T., Servranckx, R., Yue, G., Trickl, T., Sica, R., Doucet, P., and Godin-Beekmann, S.: The untold story of pyrocumulonimbus, B. Am. Meteorol. Soc., 91, 1193–1209, 2010.

Fromm, M., McRae, R., Sharples, J., and Kablick, G.: Pyrocumulonimbus pair in wollemi and blue mountains national parks, 22 November 2006, Aust. Meteorol. Oceanogr. J., 62, 117–126, 2012.

Haines, D. A.: A lower atmosphere severity index for wildland fires, National Weather Digest, 13, 23–27, 1988.

Jost, H.-J., Drdla, K., Stohl, A., Pfister, L., Loewenstein, J. P., Hudson, P. K., Murphy, D. M., Cziczo, D. J., Fromm, M., Bui, T. P., Dean-Day, J., Gerbig, C., Mahoney, M. J., Richard, E. C., Spichtinger, N., Pittman, J. V., Weinstock, E. M., Wilson, J. C., and Xuerei, I.: In-situ observations of mid-latitude forest fire plumes deep in the stratosphere, Geophys. Res. Lett., 31, L11101, doi:10.1029/2003GL019253, 2004.

Kahn, R. A., Chen, Y., Nelson, D. L., Leung, F.-Y., Li, Q., Diner, D. J., and Logan, J. A.: Wildfire smoke injection heights: two perspectives from space, Geophys. Res. Lett., 35, L04809, doi:10.1029/2007GL032165, 2008.

Lavoué, D., Liousse, C., Cachier, H., Stocks, B. J., and Goldammer, J. G.: Modeling of carbonaceous particle emitted by boreal and temperate wildfires at northern latitudes, J. Geophys. Res.-Atmos., 105, 26871–26890, 2000.

Lindley, T., Vitale, J., Burgett, W., and Beierle, M.: Proximity meteorological observations for wind-driven grassland wildfire starts on the southern high plains, Elect. J. Severe Storms Meteorol., 6, 1–27, 2011.

NHESSD
2, 7269–7292, 2014

Linking local wildfire dynamics to pyroCb development

R. H. D. McRae et al.

Mazzoni, D., Logan, J. A., Diner, D., Kahn, R., Tong, L., and Li, Q.: A data-mining approach to associating MISR smoke plume heights with MODIS fire measurements, Remote Sens. Environ., 107, 138–148, 2007.
McRae, R. and Sharples, J.: A conceptual model for assessing the risk posed by extreme bushfires, Aust. J. Emerg. Manage., 26, 47–53, 2011.
McRae, R. and Sharples, J.: A process model for forecasting conditions conducive to blow-up fire events, Proceedings, 2013 MODSIM Conference, Adelaide, SA, 2013.
Mills, G. A.: On the sub-synoptic scale meteorology of two extreme fire weather days during the Eastern Australian fires of January 2003, Aust. Meteorol. Mag., 54, 265–290, 2005.
Mills, G. A.: Abrupt surface drying and fire weather Part 2: a preliminary synoptic climatology in the forested areas of southern Australia, Aust. Meteorol. Mag., 57, 311–328, 2008.
Mills, G. A. and McCaw, L.: Atmospheric stability environments and fire weather in Australia – extending the Haines index, CAWCR Technical Report 20, Centre for Australian Weather and Climate Research, Melbourne, Victoria, 2010.
Nairn, G.: A Nation Charred: Inquiry into the Recent Australian Bushfires, The Parliament of the Commonwealth of Australia, Canberra, 2003.
New South Wales Rural Fire Service: Wollemi western division section 44 report, New South Wales Rural Fire Service, Sydney, New South Wales, 2006.
Noble, I. R., Bary, G. A. V., and Gill, A. M.: McArthur's fire-danger meters expressed as equations, Aust. J. Ecol., 5, 201–203, 1980.
Potter, B. E.: A dynamics based view of atmosphere-fire interactions, Int. J. Wildland Fire, 11, 247–255, 2002.
Potter, B. E., Charney, J. J., Heilmen, W. E., and Bian, X.: Advances in fire convection dynamics, in: Advancing the Fundamental Sciences: Proceedings of the Forest Service National Earth Sciences Conference, edited by: Furniss, M., Clifton, C., and Ronnenberg, K., San Diego, CA, 18–22 October 2004, PNWGTR-689, US Department of Agriculture, Forest Service, Pacific Northwest Research Station, Portland, OR, 2007.
Rosenfeld, D., Fromm, M., Trentmann, J., Luderer, G., Andreae, M. O., and Servranckx, R.: The Chisholm firestorm: observed microstructure, precipitation and lightning activity of a pyro-cumulonimbus, Atmos. Chem. Phys., 7, 645–659, doi:10.5194/acp-7-645-2007, 2007.
Sharples, J. J.: An overview of mountain meteorological effects relevant to fire behaviour and bushfire risk, Int. J. Wildland Fire, 18, 737–754, 2009.

NHESSD
2, 7269–7292, 2014

Title Page
Abstract | Introduction
Conclusions | References
Tables | Figures
◄◄ | ►►
◄ | ►
Back | Close
Full Screen / Esc
Printer-friendly Version
Interactive Discussion

Sharples, J. J. and Matthews, S.: Evaluation of some simplified models for predicting the moisture content of fine, dead fuels, in: MODSIM2011, 19th International Congress on Modelling and Simulation, edited by: Chan, F., Marinova, D., and Anderssen, R. S., Modelling and Simulation Society of Australia and New Zealand, December 2011, Perth, Western Australia, 242–248, 2011.

Sharples, J. J. and McRae, R. H. D.: Evaluation of a very simple model for predicting the moisture content of eucalypt litter, Int. J. Wildland Fire, 20, 1000–1005, 2011.

Sharples, J. J., McRae, R. H. D., Weber, R. O., and Gill, A. M.: A simple index for assessing fuel moisture content, Environ. Modell. Softw., 24, 637–646, 2009.

Sharples, J. J., Mills, G. A., McRae, R. H. D., and Weber, R. O.: Foehn-like winds and elevated fire danger conditions in south-eastern Australia, J. Appl. Meteorol. Clim., 49, 1067–1095, 2010.

Sharples, J. J., McRae, R. H. D., and Wilkes, S. R.: Wind–terrain effects on the propagation of wildfires in rugged terrain: fire channelling, Int. J. Wildland Fire, 21, 282–296, 2012.

Smith, R.: Report of the Key Issues Identified from Operational Reviews of Major Fires in Victoria 2006/07, Department of Sustainability and Environment, Melbourne, 2007.

Steiner, J. T.: Blow-up fires – the Byram wind profile, Aust. Meteorol. Mag., 24, 139–142, 1976.

Teague, B., McLeod, R., and Pascoe, S.: 2009 Victorian Bushfires Royal Commission Final Report, State of Victoria, Melbourne, Victoria, 2010.

Trentmann, J., Luderer, G., Winterrath, T., Fromm, M. D., Servranckx, R., Textor, C., Herzog, M., Graf, H.-F., and Andreae, M. O.: Modeling of biomass smoke injection into the lower stratosphere by a large forest fire (Part I): reference simulation, Atmos. Chem. Phys., 6, 5247–5260, doi:10.5194/acp-6-5247-2006, 2006.

Val Martin, M., Logan, J. A., Kahn, R. A., Leung, F.-Y., Nelson, D. L., and Diner, D. J.: Smoke injection heights from fires in North America: analysis of 5 years of satellite observations, Atmos. Chem. Phys., 10, 1491–1510, doi:10.5194/acp-10-1491-2010, 2010.

Table A1. List of events in Australia which, based on available evidence, are known to have been, or are strongly suspected to have been, pyroCb occurences.

Year	Date	State	Location/Fire	Longitude (°)	Latitude (°)
1995	25 Feb	Vic	Berringa	143.7	−37.8
1998	2 Jan	Vic	Caledonia River	146.8	−37.5
2001	18 Jan	WA	Splinter Rock	122.9	−33.1
2002	17 Dec	Victoria	Big Desert	141	−35.7
2003	17 Jan	ACT	Stockyard Spur	148.9	−35.5
	18 Jan	NSW	Broken Cart Fire	148.6	−35.5
	18 Jan	ACT	Stockyard Complex	148.9	−35.6
	18 Jan	ACT	Stockyard Complex	148.8	−35.5
	18 Jan	NSW	McIntyres Hut Fire	148.8	−35.3
	18 Jan	NSW	Alpine Complex	148.4	−36
	26 Jan	NSW/Vic	Alpine Complex	[147]	[−37]
	30 Jan	NSW/Vic	Alpine Complex	[148]	[−37]
2006	19 Jan	Victoria	Grampians	142.4	−37.3
	22 Nov	NSW	Wollemi	150.3	−32.8
	22 Nov	NSW	Grose Valley	150.3	−33.6
	29 Nov	NSW	Pilliga	149.2	−31
	6 Dec	Victoria	Alpine Complex	146.5	−36.8
	14 Dec	Victoria	Alpine Complex	146.2	−37.5
	16 Dec	Victoria	Alpine Complex	[147]	[−38]
2007	16 Jan	Victoria	Alpine Complex	146.4	−37.1
2009	7 Feb	Victoria	Kilmore Gap	145.1	−37.2
	7 Feb	Victoria	Murrindindi	145.5	−37.4
	7 Feb	Victoria	Bunyip	145.7	−37.9
	7 Feb	Victoria	Beechworth	146.7	−36.4
2010	18 Feb	WA	Esperance	122.2	−33.1
2012	18 Oct	WA	Deserts	125.1	−27.3
	18 Oct	WA	Deserts	124.8	−26.5
	18 Oct	WA	Deserts	126.7	−27.4
	18 Oct	WA	Deserts	126	−27.6
	18 Oct	WA	Deserts	126.7	−28.3
	29 Oct	WA	Deserts	122.8	−28.5
2013	4 Jan	Tasmania	Dunalley	147.7	−42.9
	13 Jan	NSW	Wambelong	149	−31.3
2014	16 Jan	Victoria	Grampians	142.4	−37
	17 Jan	Victoria	Grampians	142.3	−37.1
	9 Feb	Victoria	East Gippsland	145.5	−37.3

Note that geographic coordinates are accurate to 0.1° only, and those in brackets are approximate.

NHESSD
2, 7269–7292, 2014

Linking local wildfire dynamics to pyroCb development

R. H. D. McRae et al.

Table A2. List of events in Australia which are currently under investigation as candidates for pyroCb occurences.

Year	Date	State	Location/Fire	Longitude (°)	Latitude (°)
1983	16 Feb	Vic/SA	Ash Wednesday	[144]	[−38]
1994	23 Jan	WA	WSW of Kalgoorlie	[120]	[−32]

Note that geographic coordinates are accurate to 0.1° only, and those in brackets are approximate.

NHESSD
2, 7269–7292, 2014

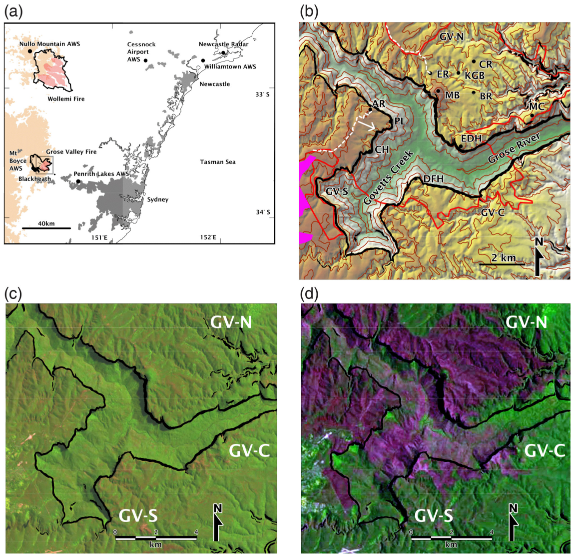

Figure 1. (a) Location map, showing: urban areas (grey), areas above 800 m a.s.l. (orange), burnt areas (black outline) and blow-up fire events (red). Also shown is the extent of the other figure panels. **(b)** Localities for the Grose Valley Fire. The outskirts of the town of Blackheath (lower left) are shown in magenta, while the final fire area is outlined in red. The contour interval is 100 m, major clifflines are shown by heavy black lines. Elevation colours: 300 m = green; 600 m = white; 800 m = yellow; 1100 m = brown. The three fire areas are labelled GV-N, GV-C and GV-S. Locality codes are – AR: Anvil Rock; BR: Banks Ridge; CH: Clarke Head; CR: Carmarthen Ridge; DFH: Du Faur Head; EDH: Edgeworth David Head; ER: Explorers Range; KGB: King Georges Brook; MB: Mt Banks; MC: Mt Caley; PL: Perrys Lookdown. The white dashed lines are the easterly containment lines early on 22 November. **(c)** Landsat imagery from 2002. **(d)** Landsat imagery from 5 weeks after the Grose Valley Fire. The intensity of the red is a measure of fire intensity. (Landsat 5 Thematic Mapper, Path 9 Row 83, 27 December 2006.) Major clifflines are highlighted in **(c)** and in **(d)**.

NHESSD
2, 7269–7292, 2014

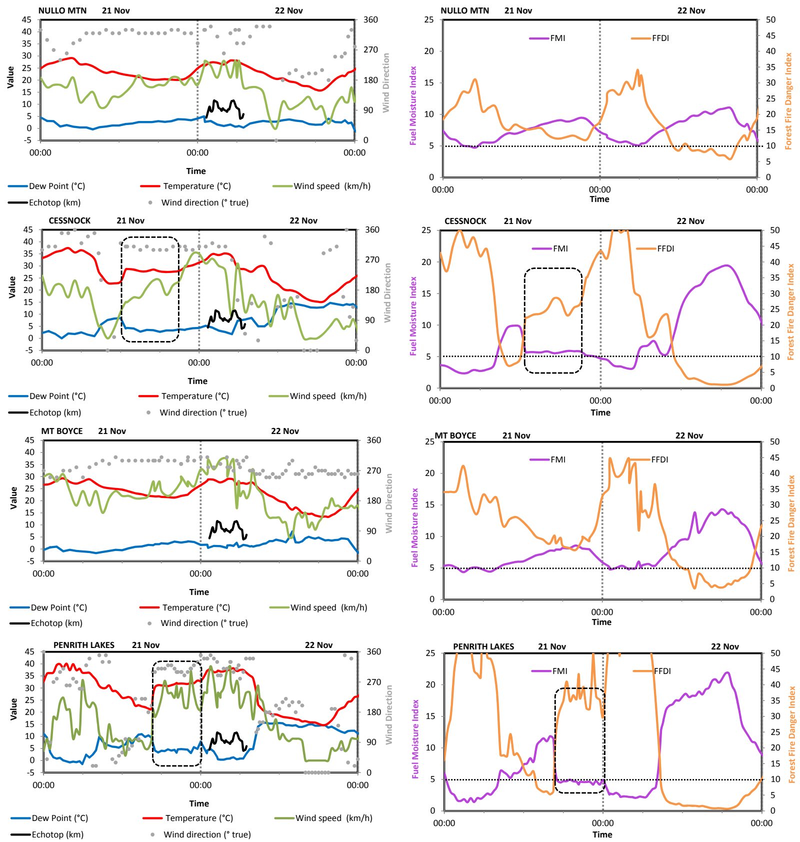

Figure 2. Weather graphs for four AWSs in the region, with surface weather (left-hand panels) and fire weather (right-hand panels). Dotted horizontal lines indicate FMI = 5. For Cessnock and Penrith Lakes, the black dotted outlines highlight the nocturnal foehn event. The echotop time sequence (see Fig. 4 for detail) is included for cross-reference purposes.

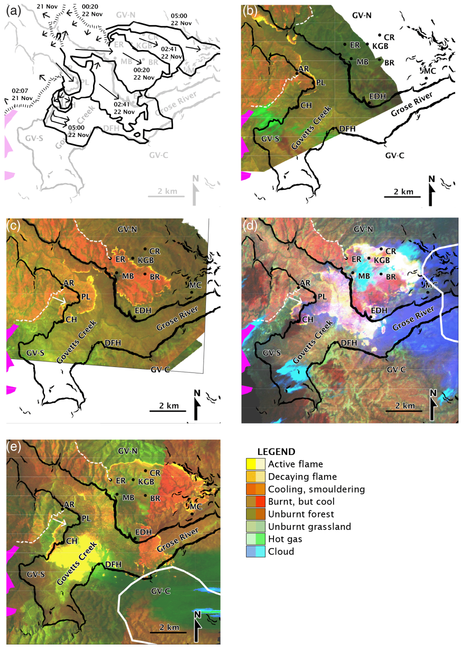

Figure 3. (a) Summary of Grose Valley Fire spread dynamics. Arrows show, in a stylised manner, fire spread directions. Cross-hatched lines indicate the control lines that were in place from time-to-time. (**b**, **c**, **d** and **e**) Linescan excerpts. Control lines are shown by white dashed lines. **(b)** Run 116, flown 02:07, 21 November. **(c)** Run 117 M, flown at 00:20, 22 November. The white arrow near PL is the critical point where fire was able to spread along the cliff-top into the GV-S area. **(d)** Run 126, flown at 02:41, 22 November. The core of the contemporaneous radar reflectivty pattern is outlined in white. **(e)** Run 127 M, flown at around 05:00, 22 November. The core of the contemporaneous radar reflectivty pattern is outlined in white. **(f)** Linescan thematic legend – note the colours are indicative only, as there is considerable variation due to smoke density. Some colours arise from a composite of surface and atmospheric features.

NHESSD
2, 7269–7292, 2014

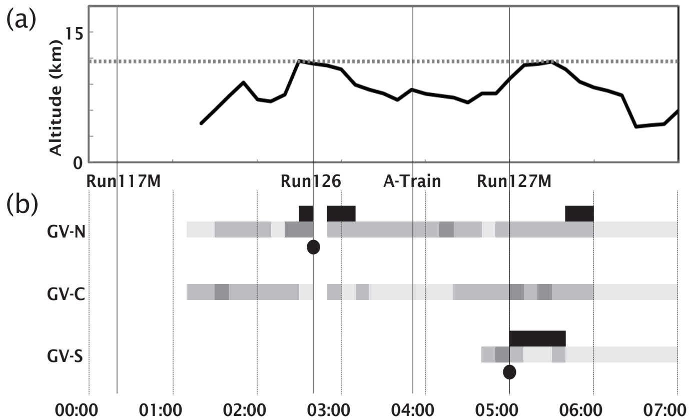

Figure 4. Time series analysis of localised convective activity from radar data. The dataset spans 00:00 and 07:00 on 22 November only. **(a)** Echotop time series, from Newcastle radar data, for Grose Valley Fire. **(b)** Radar summaries. Black bars indicate pyro-tops over 9 km a.s.l. Grey bars represent ten minute typical reflectivity, with the grey shade indicating reflectivity class values. Vertical black lines indicate key overhead remote sensing passes. The black dots indicate identified fire channelling events.

NHESSD

2, 7269–7292, 2014

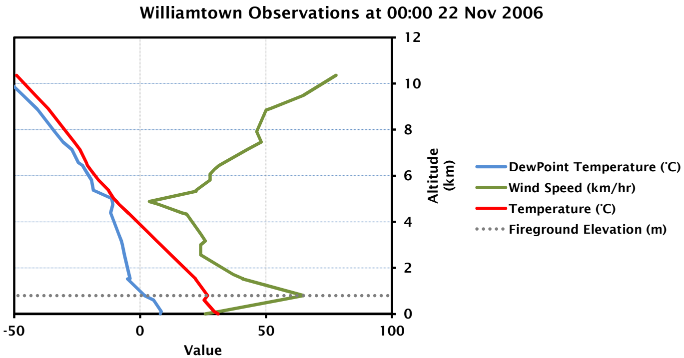

Figure 5. Radiosonde data from Williamtown, 00:00 22 November. The grey line indicates the elevation of the GVN fire area.

NHESSD
2, 7269–7292, 2014

Linking local wildfire dynamics to pyroCb development

R. H. D. McRae et al.

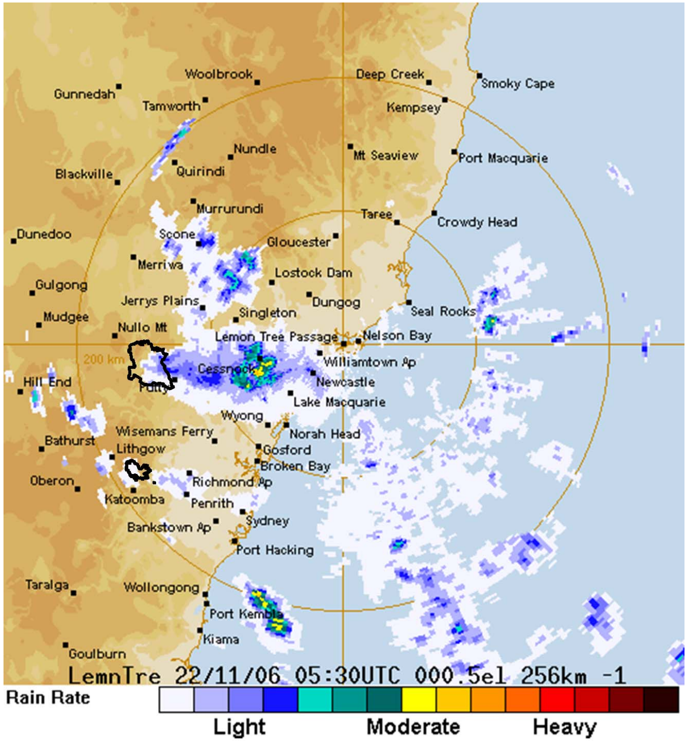

Figure 6. Newcastle (Lemon Tree Passage) Radar reflectivity product for 04:40 22 November. The black outlines are the burnt areas. The diagonal band of instability that is about to pass over the radar site is strongly interacting with the plume from the Wollemi Fire, between Putty and Nullo Mountain.

NHESSD
2, 7269–7292, 2014

Title Page
Abstract | Introduction
Conclusions | References
Tables | Figures
◀| |▶
◀ ▶
Back | Close
Full Screen / Esc
Printer-friendly Version
Interactive Discussion